DEVELOPMENT OF ULTRA LOW PHASE NOISE X-BAND OSCILLATORS

R. Boudot *, S. Gribaldo †, Y. Gruson *, N. Bazin *, E. Rubiola *, O. Llopis †, and V. Giordano *

*Dpt. LPMO Institut FEMTO–ST
UMR 6174 CNRS – Université de Franche–Comté
32 av. de l'Observatoire, 25044 Besançon Cedex, France
Email : rodolphe.boudot@femto-st.fr

†LAAS–CNRS
7 av. du Colonel Roche, 31077 Toulouse, France

Abstract— **This paper reports on the design and the measurement of low phase noise X-band oscillators combining a room temperature high-Q whispering gallery mode (WGM) sapphire resonator and an ultra-low phase noise sustaining amplifier. The resonator thermal configuration has been optimized leading to a thermal frequency sensitivity of -0,05 ppm/K. Compact microstrip DBR (Dual Behavior Resonators) filters have been realized to suppress cavity spurious modes. High performance commercially available amplifiers have been tested. Owing to the low phase noise, the measurement of oscillators requires cross-correlation and some unusual solutions. X-band oscillators typical phase noise as low as -36 dB.rad^2.Hz at 1 Hz Fourier frequency, -145 dB.rad^2/Hz at 10 kHz offset and -160 dB.rad^2/Hz at 100 kHz from the carrier have been measured. Parallely, two excellent and original double stage amplifiers based on a Si-SiGe transistors cascade (Power gain=8.2 dB - Phase noise performances : -168 dB.rad^2/Hz at 100kHz offset) have been designed, precisely modelled (non-linear and noise modelling) and optimized thanks to dedicated CAD techniques.**

I. INTRODUCTION

Advances in the performances of microwave sources, especially in reducing their phase and amplitude fluctuations, results in important improvements in a growing number of scientific and technical applications. For example, besides any reduction in oscillators phase noise will improve Doppler radar systems sensitivity. Apart from commercial and military uses, high spectral purity microwave oscillators play also a fundamental role in time and frequency metrology and precise physical experiments. Thus, phase noise performances as low as - 140 dB.rad^2/Hz at 10kHz from an X-band carrier are typically required for such applications. The Microwave WGM Sapphire Resonator, permitting to obtain high-Q factors (200.000 at 300K), constitutes an excellent frequency reference to develop microwave oscillators. Thus, phase noise performances as low as - 167 dB.rad^2/Hz at 10 kHz offset from an X-band carrier [1] have been already demonstrated, yet using a cumbersome interferometric correction technique. Another technique consists to combine the WGM sapphire resonator with an ultra low phase noise amplifier. Using this topology, the phase noise of a room temperature 4.8 GHz oscillator based on a SiGe bipolar transistor was reduced to -135 dB.rad^2/Hz at 1kHz Fourier frequency [2]. The gain-phase noise tradeoff is a major issue in the oscillator design. In the X-band range, this problem may be difficult to overcome with a single stage SiGe amplifier approach because the power gain is not sufficient. Our solution, inspired of [2], consists of using multi-stage SiGe HBT amplifiers, which show lower phase noise than the traditional AsGa devices.

In the first part of this paper, the main characteristics of the WGM sapphire resonator are described. The configuration of sapphire resonators we use is explained. Their thermal stabilization is based on the use of an original symmetrical duralumin cavity coupled to a high-precision electronic temperature controller [3]. The main drawback of the outer cavity is that it interacts with the sapphire rod, giving rise to a number of low-Q spurious resonances at unpredictable frequencies. As a consequence, the realization of microwave DBR filters, whose principle is explained, has been necessary to supress undesired modes. The different steps of their design and their performances are shown.

The second part is devoted to describe mechanisms responsible for the sustaining amplifier phase noise. Indeed, one of the possible approach to optimize the oscillator phase noise is to focus on the amplifier included in the feedback loop. As described in Leeson's model [4], the amplifier phase fluctuations are converted into oscillator frequency fluctuations inside the resonator bandwidth. Using SiGe transistors, several cascaded amplifying stages are needed to obtain sufficient gain performances in the X-band range. Phase noise of commercial amplifiers has been characterized with a high sensitivity noise measurement system (NMS) based on carrier suppression techniques.

The third section of this article is devoted to present the oscillators design. Commercial AML amplifiers have been used. An unusual specific cross-correlation measurement bench has been mounted. Oscillators phase noise performances are shown and discussed.

In a fourth and last part, two "home-designed" double stage amplifiers, using a Si-SiGe cascade, are introduced. The non-linear and noise modelling of these devices is explained.

1-4244-0074-0/06/$20.00 © 2006 IEEE.

Phase noise of these amplifiers is simulated using dedicated techniques and compared to experimental measurements.

II. The WGM sapphire resonator and its environment

A. Description

The heart of our oscillators consists of a room temperature low-cost Verneuil cylindrical sapphire resonator machined as a Al_2O_3 single crystal c-axis oriented rod. This resonator is 34.10 mm in diameter and 17.05 mm high and operates in the WGM configuration. The propagation of these high order modes, near the curved air-dielectric interface, is a similar phenomenon to light propagation in optic fibers. Whispering gallery modes permit a great confinement of electromagnetic energy essentially limited by dielectric losses. As a consequence, Q factors as high as 2.10^5 at 300K can be obtained [5]. This electromagnetic configuration allowed us to drill a 3-mm diameter hole in the center of the crystal. Thus, the resonator is enclosed in a cylindrical duralumin 68.20×34.10 mm^2 cavity to limit radiation losses, ensure a primary thermal shielding and enable a rigid and stable mechanical mounting. In each oscillator described in this paper, quasi-transverse magnetic whispering gallery (WGH) modes are excited with straight antenna coupling probes.

B. Spurious mode suppression : design of bandpass DBR Filters

The use of the metallic cavity makes arise numerous undesirable low-Q spurious modes, inducing a degradation of the main resonance Q-factor. A method [6] for suppressing these spurious resonances at room temperature has already been successfully tested on several sapphire resonators in FEMTO-ST. This technique consists in depositing thin Cr lines on the top surface of the resonator in order to affect modes whose electromagnetic fields configuration don't present the same periodical variations along azimuthal direction than WG modes. However, in the structure described above, this embedded modal selector was not sufficient. A microwave absorber has been added inside the cavity but the remaining spurious mode was not sufficiently altered.

To overcome this issue, the design and realization of narrow bandpass microstrip DBR filters has been undertaken to reject sufficiently undesired resonances. This filter technology has been chosen because of its low temperature sensitivity and its easy machining. Analytical models and theoretical explanations about microwave DBR filters are discussed in the literature [7]. Our generic DBR is based on the parallel association of two-different length open-circuited stubs acting as bandstop structures. Each of them brings a transmission zero depending on its fundamental resonant condition. Then, a constructive recombination between the rejected bands can be obtained. This results in a bandpass response created between the lower and upper rejected bands. A n^{th} order DBR filter is then developed by associating n generic DBR linked by $\lambda/4$ impedance inverters. For our application, using ADS Momentum simulator, we have modelled and simulated a 3^{rd} order Tchebychev filter implemented in microstrip technology on a classical alumina substrate (permittivity ε_r = 9.8 and thickness h = 254 μm). The 3 generic DBR constituting the filter have similar dimensions. They are composed of a l_{lf}-length stub (l_{lf}= 9.430 mm) creating the lower rejected band and a l_{hf}-length stub (l_{hf} = 2.309 mm) creating the upper rejected band. The main transmission line impedance is 50 Ω (line width = 238 μm) to ensure a correct impedance matching. Initially set to 238 μm, the width of stubs consituting the DBR filter has been extended to 248 μm to reduce losses. Linewidth discontinuities have been avoided to make the DBR filter tuning easier and reduce its transmission losses [7]. Then, classical photolithography and wet-etching processes have been used to realize the DBR filter. The DBR filter has then been implemented in a metallic box to enable a stable mechanical mounting. Figure 1 shows us a picture of a DBR filter realized for eliminating the spurious cavity modes.

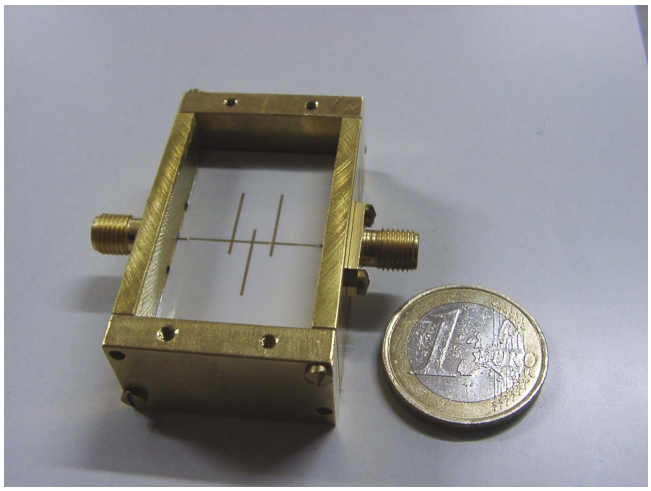

Fig. 1. *Picture of DBR filters used for the WGM sapphire resonator spurious modes suppression.*

Figure 2 shows that experimental responses agree quite well with the electromagnetic simulations despite a little frequency shift. Moreover, the experimental 4.5 dB insertion losses in the bandpass are 1 dB higher than simulated ones. These differences between simulated and experimental results are likely due to a systematic error induced by the calculation method, uncertainty about the substrate permittivity and the delicate deposit of SMA connectors. The sapphire resonator main spurious mode at 9.340 GHz is rejected at -26 dB. Concerning the development of X-band oscillators using AML commercial amplifiers (see section III-B) whose power gain is 22.5 dB, the characteristics of these DBR filters are fully satisfying.

C. The sapphire resonator thermal stabilization

At room temperature, a major drawback of the sapphire resonator is its high sensitivity to thermal fluctuations (-70 ppm/K) limiting the oscillator stability on the long term. To overcome this issue, an efficient thermal control has to be

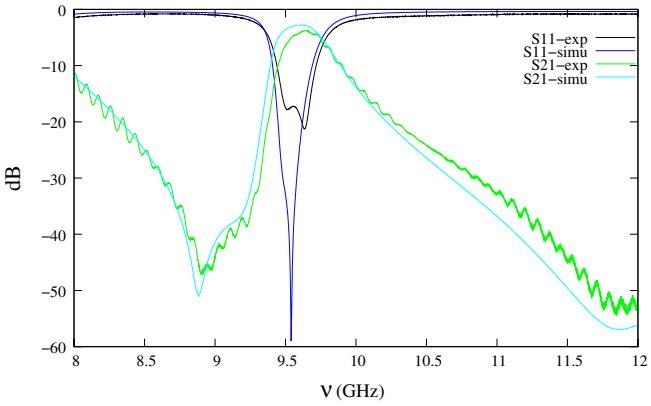

Fig. 2. *Simulated and measured S-parameters of DBR filters : . . . =S_{11} simu, – –=S_{11} exp, —=S_{21} simu, ——=S_{21} exp*

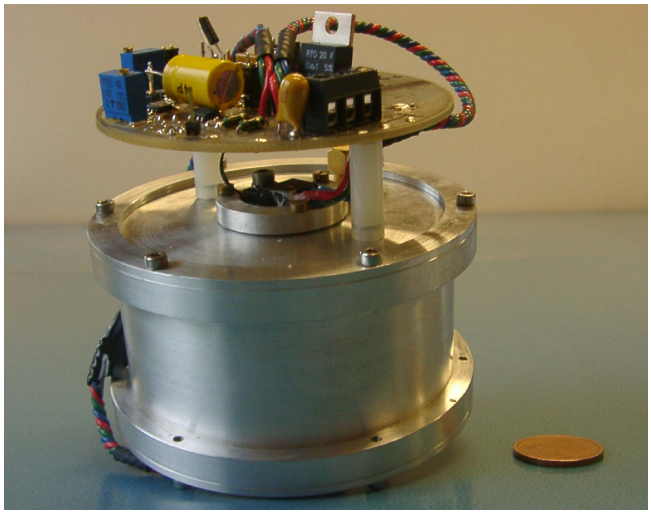

Fig. 3. *Picture of the symmetrical duralumin cavity containing the sapphire resonator and supporting the electronic temperature controller.*

implemented in order to reduce the effect of temperature variations on the resonator frequency. Obviously, temperature control at the 1 mK level that can be easily reached with classical controller is not sufficient for such metrological applications.

A few methods have been implemented by various groups to stabilize the sapphire resonator temperature near 300K. UWA (University of Western Australia) has proposed a room-temperature dual mode technique utilising a single sapphire resonator in which two orthogonally polarised whispering gallery modes are excited. Their beat frequency is compensated at the temperature where the absolute temperature coefficients of frequency of the two modes are equal. An X-band oscillator with a frequency stability of 8.10^{-12} for a 1s integration time has been experimentally achieved using this solution [8]. Nevertheless, this cumbersome method requires two Pound servo controls to optimize the long term stability of each single mode loop. It has also been proposed to use a thermal sensitive quartz oscillator as a thermal sensor [9].

The solution we propose has been explained and successfully applied on C-band resonators [3]. The main idea is to ensure as perfect as possible the symmetry of the thermal paths with respect to the electromagnetic fields configuration inside the sapphire resonator. Thus, we developed an original duralumin cavity on which is directly embedded a high-precision electronic temperature controller (figure 3). The whole assembly is then enclosed in a box containing insulating foam. The design of the cavity, compared to the one described in [3], has been improved in order to get an easier mechanical mounting.

We chose to stabilize the resonator at 313K. A model, described in [3], consisting to establish an electrical analogy of the resonator thermal behavior, has permitted us to estimate that the resonator thermal frequency sensitivity is better than -0.05 ppm/K in this optimal structure.

III. X-BAND MICROWAVE SiGe HBT AMPLIFIERS

A. Phase Noise Mechanisms

1) Additive white noise: The white noise is due to the direct superposition of the device HF noise. This "additive" process depends on the amplifier microwave input power P_{in}, the linear noise figure F and the thermal energy kT where k =1.28.10^{-23} J/K is the Botzmann constant and T =290K the reference temperature. The corresponding phase noise $S_{\varphi_0}(f)$ can be written :

$$S_{\varphi_0}(f) = \frac{FkT}{P_{in}} \tag{1}$$

The noise figure, which is typically 1-2 dB, depends on the device bandwidth, frequency and technology. A larger bandwidth induces a higher input noise and as a consequence a higher noise figure. The additive noise determines the device phase noise floor. When amplifiers are cascaded, the noise contribution of each stage is divided by the gain of all the preceding stages [10]. Thus, in most practical cases, the total noise of a multi-stage amplifier is the noise of the first stage. Obviously, this remark also holds for phase noise.

2) Flicker noise: The mechanism that originates phase flickering is a low frequency (close to DC) random process with spectrum of the flicker type that modulates the carrier. This conversion phenomenon is often called parametric noise because the near-dc flickering modulates a parameter of the device high-frequency (HF) model. This mechanism takes place through non-linear elements. It has been experimentally observed that phase flickering is about independent of the carrier power [11]. It means that the flicker noise of m identical cascaded amplifiers is about m times the noise of a single amplifier. This behavior is radically different from the additive white noise behavior. Phase flickering depends on the physical size of the amplifier active region.

3) Amplifier phase noise spectrum: Let us remember that the white noise term, noted here b_0 (where b_0= FkT/P_{in}),

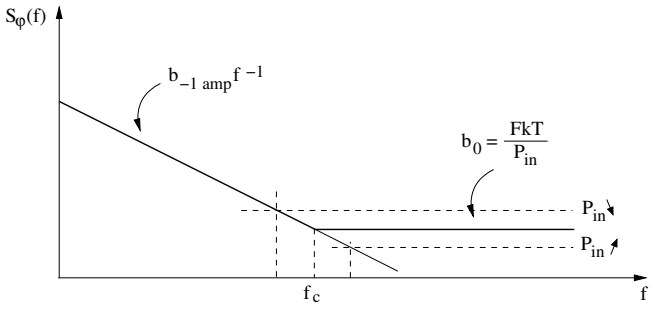

Fig. 4. *Typical phase noise of an amplifier.*

depends on the carrier input power while the flicker term $b_{-1_{amp}} f^{-1}$ does not. The amplifier phase noise spectrum is then given by adding the two contributions described above as shown on figure 4.

The frequency at which the slope changes from 0 to -1 is the corner frequency f_c, at which it holds that $b_{-1_{amp}} f^{-1} = b_0$.

4) Low phase noise X-band amplifiers: The two phase noise mechanisms described above have to be minimized to optimize the device phase noise performances. Amplifiers presenting the lowest phase noise performances on the C-band range are generally based on bipolar SiGe transistors [12]. In the X-band range, SiGe transistors power gain is strongly reduced. It then becomes a necessity in this frequency range to realize multi-stage amplifiers. The amplifier gain has to be sufficient to permit a resonator coupling for which the Q-factor is as high as possible. However, a trade-off must be found between the amplifier gain and phase noise performances.
In order to develop X-band low phase noise oscillators, high-performance commercially available amplifiers have been studied. Moreover, a "home-designed" double stage Si-SiGe amplifier has been modelled, designed, optimized and realized (see section V).

B. AML812PNB1901 comercial amplifiers study

First studies have been led on a high performance commercial amplifier (AML812PNB1901), which has a gain of 22.5 dB and a 1-dB compression output power of +17 dBm. A classical interferometer [13], shown on figure 5, has been mounted to measure their phase noise performances. In this experimental set-up, the AML amplifiers input power is P_{in}= -10 dBm. Setting the phase shifter φ_1 and the attenuator γ_1, a carrier suppression level of 70 dB is obtained at the Δ output of the hybrid. The DUT noise sidebands, which are not suppressed by the interference mechanism, are amplified by a low noise amplifier (LNA) and down converted to base band by the mixer. Setting φ_2 to 90°, the mixer down converts PM noise. A bandpass filter (bandwidth : 300 MHz) is used to limit noise integrated over the amplifier large bandwidth (8-12 GHz).

Figure 6 shows the measured phase noise of a single AML amplifier. The spectrum indicates that b_0 = -155 dB.rad^2/Hz and $b_{-1_{amp}}$ = -128.4 dB.rad^2/Hz. At the frequency f_c, the

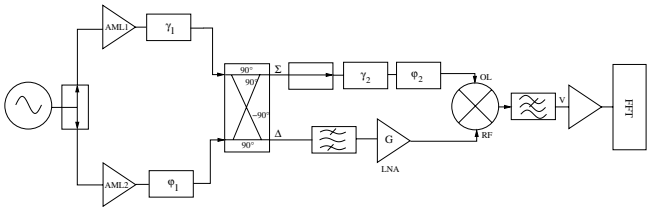

Fig. 5. *Interferometer to measure AML amplifiers phase noise*

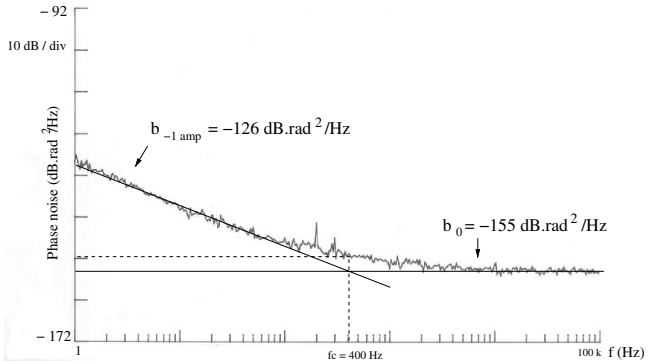

Fig. 6. *Phase noise of a AML amplifier (P_{in} =-10 dBm).*

asymptotic approximation is some 3 dB lower than the measured spectrum as expected. The amplifier phase noise floor being additive, phase noise floors as low as -160 dB.rad^2.rad^{-1} should be measured at higher input power (P_{in} = -5 dBm).

IV. X-BAND LOW PHASE NOISE OSCILLATORS

A. Oscillators design using AML amplifiers

X-band oscillators we developed are based on a parallel feedback topology. The oscillator loop consists of a 313K temperature controlled sapphire resonator, a low phase noise microwave amplifier (AML812PNB1901 : 22.5 dB gain and +17 dBm output power), two isolators, a bandpass filter and a coupler to extract the signal. Concerning each resonator, a $WGH_{8,0,0}$ mode (9.512 GHz for the first oscillator and 9.518 GHz for the second one) is excited. The loaded Q-factor is 80.000, thus the Leeson frequency $f_L = \frac{\nu_0}{2Q_L}$ is 60 kHz. The resonator transmission losses are 11.5 dB. The coupling coefficients are β_1= -3.6 dB and β_2= -4.5 dB.
The sustaining amplifier is operated in soft compression to optimize the device phase noise floor performances as shown in relation (1).

B. Phase noise measurement

The expected phase noise is lower than that of tunable sources, like microwave synthesizers, and also lower than the background noise of sophisticated instruments, as the dual-channel delay-line homodyne [14]. In addition, for technical reasons it is virtually impossible to manufacture two resonators whose pass bands overlap. As a consequence, it's impossible to phase-lock two oscillators and measure the error signal fluctuations. It's also impossible to design a homodyne system

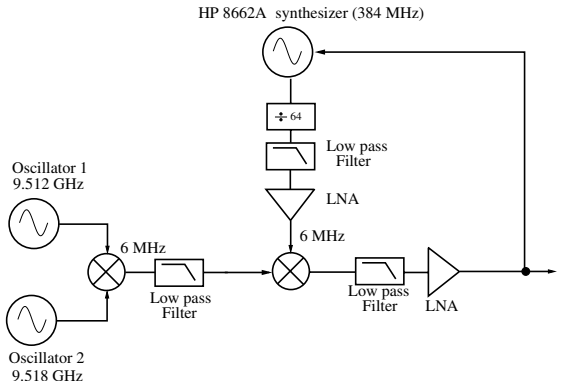

Fig. 7. *First phase noise measurement bench.*

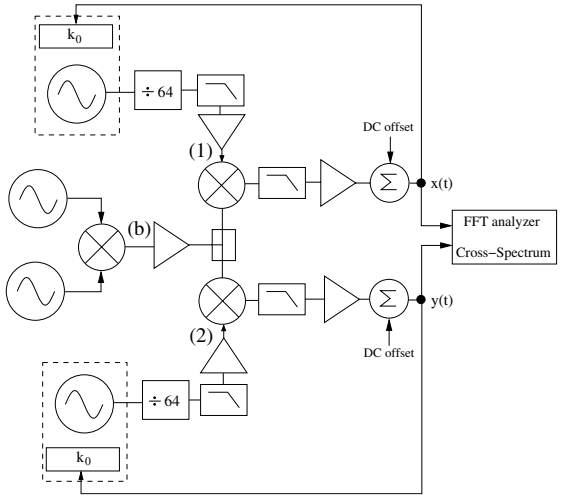

Fig. 8. *Cross-correlation measurement bench.*

using a resonator as a frequency discriminator. Thus, we studied the 6 MHz beat signal b between two quasi-identical sapphire oscillators. In a first time, the beatnote has been compared to a 384 MHz reference synthesizer (HP8662A) divided by 64 as shown on figure 7. However, we observed that oscillators phase noise was still too low to be measured. The measurement was clearly limited by the HP8662A synthesizer noise above 10 kHz.

Therefore, a specific cross-correlation measurement bench (figure 8) has been mounted to measure oscillators phase noise.

As shown on figure 8, this method consists in locking oscillators 1 and 2 (384 MHz HP8662A synthesizers divided by 64) on the 6 MHz sapphire oscillators beat signal b using phase lock loops (PLLs). Outside of the PLLs bandwidth, the error voltages are $x = k_\phi(\phi_b - \phi_1)$ and $y = k_\phi(\phi_b - \phi_2)$, where k_φ= 0.35V/rad is the sensitivity of the saturated mixer. An estimation of the crosscorrelation function between x and y, considering a finite integration time T, is given by :

$$C_{x,y}(\tau) = \frac{1}{T}\int_t^{t+T} [\phi_1(t) - \phi_b(t)][\phi_2(t-\tau) - \phi_b(t-\tau)]dt \quad (2)$$

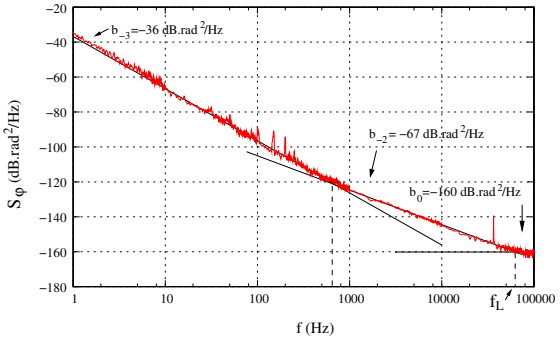

Fig. 9. *Phase noise of a X-band sapphire oscillator using AML amplifier.*

With the hypothesis of independant phase fluctuations of the 3 oscillators, all the crosscorrelation terms cancel with infinite or at least large integration times. Thus, only remains a term proportionnal to the autocorrelation function $C_{bb}(\tau)$ of the tested beatnote b, from which can be extracted by Fourier Transform its phase noise spectral density.

The hypothesis of statistical independence deserves further attention. In fact, the mixer offset is sensitive to microwave power, for the AM noise turns into dc noise in x and y. In the case of the beat note this effect is fully correlated, for it is not rejected. However a second-order effect, it shows up because the detection mechanisms gets a small correlated random signal out of large noise. Different papers in the literature [15], [16] show the existence of an optimal working point, distinct of the quadrature condition, for which the mixer sensitivity to amplitude fluctuations is minimum and which has to be determined experimentally. In our experimental set-up, no such sweet point has been detected in the range where the mixer phase sensitivity is still maximum.

The oscillators phase noise spectrum obtained correlating well with AML amplifiers performances given in [17] and the Leeson's model, we did not investigate further on the AM noise.

Figure 9 shows the phase noise of a single oscillator assuming that it's 3 dB lower than the oscillator pair. A model that has been useful to describe the oscillator noise spectra is the power law [18] :

$$S_\varphi(f) = \sum_{i=0}^{-4} b_i f^i \quad (3)$$

Concerning the oscillators described above, we obtain b_{-3}= -36 dB.rad^2/Hz , b_{-2}= -67 dB.rad^2/Hz, and b_0= -160 dB.rad^2/Hz.

One can estimate the X-band sapphire oscillator Allan variance $\sigma_y(\tau)$ from the white and flicker frequency noise using the equation :

$$\sigma_y^2(\tau) = \frac{b_{-2}}{\nu_0^2}\frac{1}{2\tau} + 2ln2\frac{b_{-3}}{\nu_0^2} \quad (4)$$

leading to :

$$\sigma_y(\tau) = \frac{1.31.10^{-12}}{\sqrt{\tau}} + 2.35.10^{-12} \quad (5)$$

V. Design of X-band double stage amplifiers

A. Non-linear Modelling

If the amplifier is designed using discrete devices (transistors), it should be possible to predict the amplifier phase noise from the transistors $1/f$ noise and HF noise data using CAD software.

To this purpose, a nonlinear model of the transistor must be available. Such a model can be extracted from the measurement, combining the information of *DC* $I(V)$ curves and high frequency S parameters data. It is then verified using the ouput power versus input power measurement at a given microwave frequency, including the higher harmonics for a better accuracy. Fig. 10 shows such a comparison obtained for a $BFP620$ device (Infineon SiGe HBT), with a fundamental frequency of 3.5 GHz.

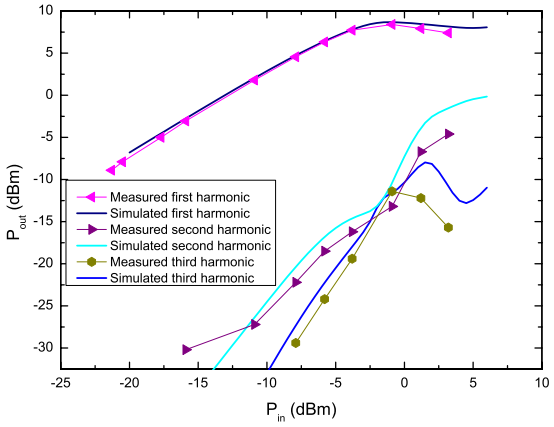

Fig. 10. *Comparison between model and measurement TB1 output power Pout vs. input power Pin (Vce = 2V and Ic= 10 mA).*

This nonlinear modelling is performed thanks to Agilent ADS software and a Gummel-Poon transistor model [19].

B. Transistor noise modelling

The two noise contributions in the device have been simulated using different techniques.

Concerning the additive phase noise, two approaches can lead to accurate results. The first one is based on the measuring of the nonlinear noise figure using a dedicated measurement bench [20].

However this approach does not allow the noise figure optimization, when a multi-impedance technique is available on the nonlinear measurement bench (under development at LAAS). The other approach is directly based on the extracted transistor model, adding to this model the classical HF noise sources : resistors thermal noise ($4kTR$) and junctions shot noise ($2qI$). The nonlinear noise simulation tool of Agilent ADS is then used to calculate the carrier to noise ratio, and thus the phase noise. We have found a relatively good agreement between these two approaches, which has to be related to the transistor model quality.

Identifying the noise sources in a transistor is a more difficult task. Moreover, active device electrical models are often far from device physics, and finding the right location in the model of a given $1/f$ noise source is almost impossible. Locating the noise sources is however essential to simulate the phase noise because, in nonlinear operation, the classical equivalent noise source approach is not valid. The noise source can be associated to a nonlinear element of the equivalent circuit [21], or considered itself as nonlinear [22].

Our approach of the problem is a little different. It uses an extrinsic LF noise source modelling, but the effect of the large signal on these noise sources is taken into account : the device LF noise is measured under large signal conditions. This approach is not completely rigorous as explained in [23], but it is enough efficient to authorize a circuit optimization [23], [24]. An example of this type of measured data for a SiGe bipolar device is depicted in Fig. 11.

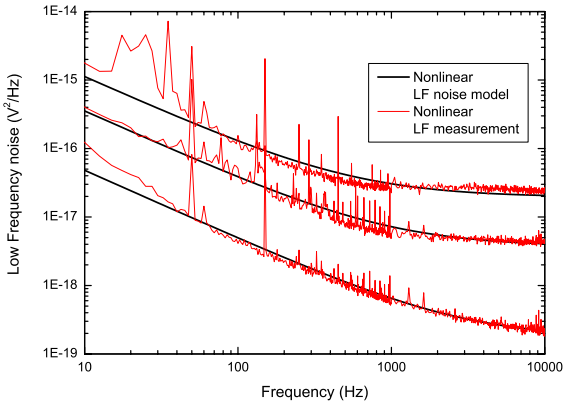

Fig. 11. *LF equivalent input voltage noise spectral density for a SiGe HBT, with input microwave power varying from 0 (quiescent device) up to 5 dBm (I_c= 10mA, V_{ce}= 2V, frequency= 5 GHz)*

The LF noise increase with the microwave power is modeled thanks to two empirical functions of the microwave power P_{in}. Adding this "nonlinear" noise source to the transistor nonlinear electrical model allows us to simulate both amplifier and oscillator phase noise.

C. Phase noise simulations and measurements

The above described nonlinear model is implemented on a commercial software : Agilent ADS.
Various approaches may be used on ADS to simulate phase noise. However, many of these tools are restricted to oscillator simulation ("pnmx" and "pnfm") and special techniques must

be implemented to simulate amplifier phase noise (particularly the $1/f$ contribution). A simple but efficient one is the quasi-static perturbation technique, which consists in introducing a small static voltage (or current) shift to evaluate the effect of a LF voltage (or current) noise on the phase of the microwave signal through the amplifier.

The conversion noise has been simulated using this technique and the ADS nonlinear noise tool has been used to compute the additive HF noise floor. Fig. 12 demonstrates that a good agreement between measurements and simulation is obtained for a transistor. The device residual phase noise is measured using previously described techniques [20], [24].
With such a modeling approach, it is possible not only to predict an oscillator phase noise, but also to optimize both the amplifier phase noise and the oscillator phase noise.

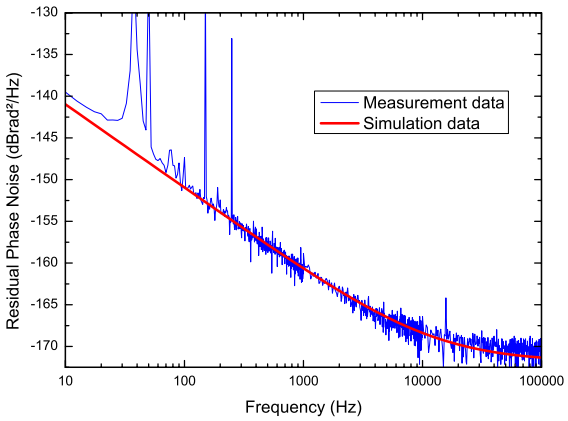

Fig. 12. *Comparison between measurement and model phase noise data for an input power of 0 dBm at 3.5 GHz.*

Considering a 6 dB losses coupling ($Q_L = \frac{Q_0}{2}$), which is an optimum coupling both for additive phase noise [25] or conversion phase noise [24] contributions in a single stage amplifier oscillator, the necessary amplifier small signal gain should be about 9 dB to take into account addtional circuit losses. This gain requirement is easy to fulfill in the low microwave range, but becomes more difficult to reach at higher frequencies (10 GHz).
The transistor small signal gain matching is indeed one of the worse loading conditions to get a low phase noise amplifier [26]. Therefore, a low phase noise two stages amplifier has been designed and features very promising performances [23].

D. Spurious oscillations

Many stability's issues appears with such a configuration. The matching between the two stages is the main cause of instability. It is necessary to simulate this behaviour together with the gain and phase noise performances.

Firstly, the bias access must be calculated in order to filter all the frequencies where a possible oscillation may occur. Then the stability factor of the amplifier is studied, and the possible oscillations in the RF range (between 10 MHz and 10 GHz) are removed using additional capacitive elements or wire bondings(particularly at the inter-stage level). Thanks to these precautions, a first X band amplifier has been succesfully designed, featuring 8.5 dB gain. This amplifier is presented on Fig. 13.

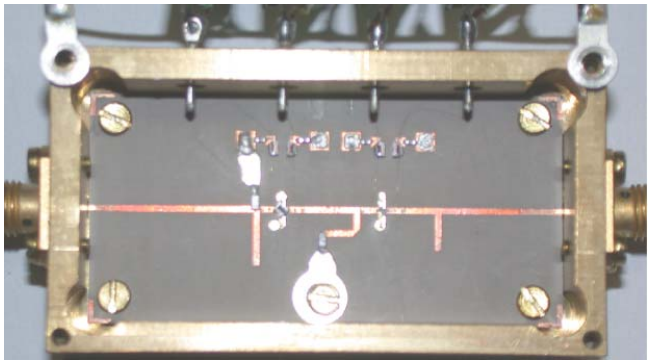

Fig. 13. *Picture of the double stage Si-SiGe amplifier with stability optimizations.*

The first results are presented on the following section.

E. Two stage amplifier preliminary results

Fig. 14 shows the preliminary phase noise result obtained with our 8.5 dB amplifier. This measurement was obtained with an input power of 0 dBm and was performed at the operation frequency of 10 GHz.

Even if a difference is obeserved between theory and experiment at low frequency offsets, the amplifier phase noise has been well predicted by the simulation. However, this circuit is still subject to instability problems (depending on the bias point) and a new design has started to overcome these problems.

VI. Conclusions

Based on a simple design, ultra low phase noise X-band oscillators, presenting phase noise performances as low as -160 dB.rad^2.Hz^{-1} at 100 kHz offset and -145 dB.rad^2.Hz^{-1} at 10 kHz offset, have been constructed. These performances are remarkable. Some techniques permit the achievement of lower phase noise levels but at the cost of a more complex and bulky system. In our case, better results would have been obtained using HEMEX sapphire crystals whose unloaded Q-factors can reach $1.9.10^5$ at 300K [27] or by cooling the resonator. Oscillators should be constructed in a near future to further validate "home-designed" amplifiers excellent performances.

VII. Acknowledgments

This research was supported by the Délégation Générale de l'Armement (DGA). We would also like to thank Dr. C.

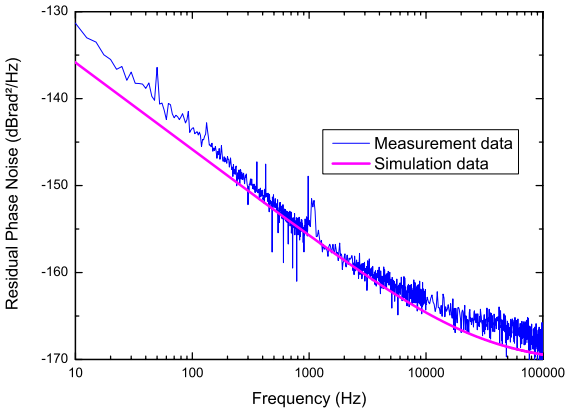

Fig. 14. *Comparison between measurement and model phase noise data for an input power of 0 dBm at 10 GHz.*

Quendo (LEST : Laboratoire d'Electronique et Systèmes de Télécommunications, Brest, France) for his help to design DBR filters.

REFERENCES

[1] C. McNeilage, J. Searls, E. Ivanov, P. Stockwell, D. Green, and M. Mossamaparast, "A review of sapphire whispering gallery-mode oscillators including technical progress and future potential of the technology," *IEEE International UFFC Joint 50th Anniversary Conference - Montreal (Canada)*, pp. 210–219, June 2004.

[2] R. Boudot, S. Gribaldo, V. Giordano, O. Llopis, C. Rocher, and N. Bazin, "Sapphire resonators + SiGe transistors based ultra low phase noise microwave oscillators," *Proceedings of the IEEE IFCS-PTTI Conference*, pp. 865–871, August 2005.

[3] R. Boudot, C. Rocher, N. Bazin, S. Galliou, and V. Giordano, "High-precision temperature stabilization for sapphire resonators in microwave oscillators," *Review of Scientific Instruments*, vol. 76, no. 095110, September 2005.

[4] D. Leeson, "A simple model of feedback oscillator noise spectrum," *Proc. Letters of IEEE*, vol. 54, no. 2, pp. 329–330, 1966.

[5] V. Braginsky, V. Chenko, and K. Bagdassarov, "Experimental observation of fundamental microwave absorption in high quality dielectric crystal," *Physics Letters A*, vol. 120, no. 6, pp. 300–301, 1987.

[6] O. DiMonaco, W. Daniau, I. Lajoie, Y. Gruson, M. Chaubet, and V. Giordano, "Mode selection for a whispering gallery mode resonator," *IEE Electronics Letters*, vol. 32, no. 7, pp. 669–670, March 1996.

[7] C. Quendo, E. Rius, and C. Person, "Narrow bandpass filters using dual-behavior resonators based on stepped-impedance stubs and different-length stubs," *IEEE Transactions on Microwave Theory and Techniques*, vol. 52, no. 3, pp. 1034–1044, March 2004.

[8] J. Torrealba, M. Tobar, E. Ivanov, C. Locke, J. LeFloch, D. Cros, and J. Hartnett, "Room temperature dual-mode oscillator - first results," *IEE Electronics Letters*, vol. 42, no. 2, pp. 99–100, January 2006.

[9] Y. Kersalé, F. Lardet-Vieudrin, M. Chaubet, and V. Giordano, "Thermal stabilisation of high-Q sapphire microwave resonator using thermosensitive quartz sensor," *IEE Electronics Letters*, vol. 34, no. 8, pp. 783–784, April 1998.

[10] H. Friis, "Noise figure of radio receivers," *IEEE Transactions on Ultrasonics, Ferroelectrics and Frequency Control*, vol. 44, no. 2, pp. 326–334, October 1997.

[11] F. Walls, E. Ferre-Pikak, and S. Jefferts, "Origin of 1/f PM and AM noise in bipolar junction transistor amplifiers," *Proc. IRE*, vol. 32, pp. 419–422, 1944.

[12] G. Cibiel and et al, "Ultra low phase noise SiGe HBT – Application to a C band sapphire resonator oscillator," *Proc. IEEE Microwave Theory Tech. Symp. – Seattle, USA*, vol. 2, pp. 691–694, 2002.

[13] E. Ivanov, M. Tobar, and R. Woode, "Microwave interferometry : Application to precision measurements and noise reduction techniques," *IEEE Transactions on Ultrasonics, Ferroelectrics and Frequency Control*, vol. 45, no. 6, pp. 1526–1535, November 1998.

[14] E. Salik, E. Rubiola, N. Yu, and L. Maleki, "Dual photonic delay line cross correlation method for phase noise measurement," *Proc. of the 2004 International Frequency Control Symposium, Montral, Canada*, pp. 303–306, 2004.

[15] R. Brendel, G. Marianneau, and J. Uebersfeld, "Phase and amplitude modulation effects in a phase detector using an incorrectly balanced mixer," *IEEE Transactions on Instrumentations and Measurement*, vol. 26, no. 2, pp. 98–102, June 1977.

[16] G. Cibiel, M. Regis, E. Tournier, and O. Llopis, "AM noise impact on low level phase noise measurements," *IEEE Transactions on Ultrasonics, Ferroelectrics and Frequency Control*, vol. 49, no. 6, pp. 784–788, June 2002.

[17] http ://www.amlj.com/

[18] E. Rubiola, "The leeson effect, chapter 1," *http ://arxiv.org/abs/physics/0502143*, p. 4, 2005.

[19] G. Massobrio and P. Antognetti, "Semiconductor Device Modelling with SPICE," *McGraw-Hill Ed.*, 1993.

[20] G. Cibiel, L. Escotte, and O. Llopis, "A study of the correlation between HF noise and phase noise in low noise silicon based transistors," *IEEE Transactions on Microwave Theory and Techniques*, vol. 52, no. 1, pp. 183–190, January 2004.

[21] O. Llopis and al, "Nonlinear noise modelling of a PHEMT device through residual phase noise and low frequency noise measurements," *Proc. of the IEEE MTT Symposium*, pp. 831–834, May 2001.

[22] H. Siweris and B. Schiek, "A GaAs FET oscillator noise model with a periodically driven noise source," *Proc. EuMC*, pp. 681–686, 1986.

[23] S. Gribaldo, R. Boudot, G. Cibiel, V. Giordano, and O. Llopis, "Phase noise modelling and optimisation of microwave SiGe amplifiers for sapphire oscillators applications," *Proceedings of 14th European Frequency Time Forum – Besançon, France*, pp. 343–347, February 2005.

[24] G. Cibiel and et al, "Optimization of an ultra low phase noise sapphire SiGe - HBT oscillator using non-linear CAD," *IEEE Transactions on Ultrasonics, Ferroelectrics and Frequency Control*, vol. 51, no. 1, pp. 33–41, January 2004.

[25] J. Everard, "Low noise oscillators," *Proc. IEEE Microwave Theory Tech. Symp.*, pp. 1077–1080, 1992.

[26] M. Regis, O. Llopis, and J. Graffeuil, "Non-linear modelling and design of bipolar transistors ultra low phase noise dielectric resonator oscillators," *IEEE Transactions on Microwave Theory and Techniques*, vol. 46, no. 10, pp. 1589–1593, October 1998.

[27] J. Hartnett, M. Tobar, E. Ivanov, and J. Krupka, "Room temperature measurement of the anisotropic loss tangent of sapphire using the whipering gallery mode technique," *IEEE Transactions on Ultrasonics, Ferroelectrics and Frequency Control*, vol. 53, no. 1, pp. 34–38, January 2006.